Reactive Power Injection Strategies for Single-Phase Photovoltaic Systems Considering Grid Requirements

Yang, Yongheng; Wang, Huai; Blaabjerg, Frede

Published in:
Proceedings of the 29th Annual IEEE Applied Power Electronics Conference and Exposition, APEC 2014

DOI (link to publication from Publisher):
10.1109/APEC.2014.6803335

Publication date:
2014

Document Version
Early version, also known as pre-print

Reactive Power Injection Strategies for Single-Phase Photovoltaic Systems Considering Grid Requirements

Yongheng Yang, *IEEE Student Member*, Huai Wang, *IEEE Member*, Frede Blaabjerg, *IEEE Fellow*
Department of Energy Technology
Aalborg University
Pontoppidanstraede 101, Aalborg East DK-9220, Denmark
yoy@et.aau.dk, hwa@et.aau.dk, fbl@et.aau.dk

***Abstract*— As the development and installation of photovoltaic (PV) systems are still growing at an exceptionally rapid pace, relevant grid integration policies are going to change consequently in order to accept more PV systems in the grid. The next generation PV systems will play an even more active role like what the conventional power plants do today in the grid regulation participation. Requirements of ancillary services like Low-Voltage Ride-Through (LVRT) associated with reactive current injection and voltage support through reactive power control, have been in effectiveness in some countries. Those advanced features can be provided by next-generation PV systems, and will be enhanced in the future to ensure an even efficient and reliable utilization of PV systems. In the light of this, Reactive Power Injection (RPI) strategies for single-phase PV systems are explored in this paper. The RPI possibilities are: a) constant average active power control, b) constant active current control, c) constant peak current control and d) thermal optimized control strategy. All those strategies comply with the currently active grid codes, but are with different objectives. The thermal optimized control strategy is demonstrated on a 3 kW single-phase PV system by simulations. The other three RPI strategies are verified experimentally on a 1 kW singe-phase system in LVRT operation mode. Those results show the effectiveness and feasibilities of the proposed strategies with reactive power control during LVRT operation. The design and implementation considerations for the characterized strategies are also discussed.**

I. Introduction

The strong development of advanced power electronics technologies has shown great potential for renewable energy integration into the grid. As it is driven by an imperative demand of clean and reliable electricity generation, the penetration degree of PhotoVoltaic (PV) systems is continuously booming [1]–[5]. This makes the distributed systems highly decentralized and vulnerable, and hence it calls for advanced control strategies for the next-generation PV systems to cater for a high penetration into the grid. The measures that most countries and international committees take are in the form of issuing grid requirements or standards, which currently require the PV systems cease to energize local loads in the presence of grid abnormal conditions, e.g. voltage sags and frequency variations [6]–[10]. Those grid integration specifications are valid, since the PV systems are dominant for residential markets at present and still account for a minor share of the overall electricity generation in most countries, when compared to other renewable systems, e.g. wind turbine power systems. Thus, single-phase configurations are more common for PV applications with lower power ratings (e.g. several kW), and are typically connected to low-voltage networks. Meanwhile, it is required in those grid regulations for most systems to operate at unity power factor (or a minimum power factor, e.g. power factor ≥ 0.9) with Maximum Power Point Tracking (MPPT) control in order to extract as much energy as possible from the PV panels [7]–[9], [11]–[13].

However, the increasing adoption of PV systems also poses more challenging issues for the distributed system operators, and the entire distributed grid. For example, potential overloading impacts will appear at the distributed feeders, especially when a very high penetration level of PV systems is reached [2], [10], [14]. Due to the intermittent nature of solar PV source and the unbalance between PV supply and load demands, voltage rise has been mostly observed in recent studies [4], [10], [15]–[19]. One possibility to mitigate voltage rises can be achieved by limiting the maximum feed-in power from PV systems or by reducing the PV penetration into the grid. However, these solutions are against the goal of carbon reduction within Europe and especially Germany and Italy by enabling an even more wide-scale adoption of renewable energies. Therefore, specific grid requirements, regarding reactive power control, have been put forward in those countries where the PV systems take a large proportion of electricity generation. It has been shown in those grid codes that the PV systems should be able to participate in voltage regulation through reactive power control (injecting or absorbing reactive power) [20], [21].

Meanwhile, owing to anti-islanding protection required by current grid codes (e.g. IEEE Std 1547-2000), the trip-off of a considerable amount of PV systems unintentionally will further induce frequency instability (grid variations) [10], [19], leading to more serious events, e.g. power outage and voltage flickering. Consequently, the realization of frequency support by means of active power curtailment is required for the PV systems. Another feature related to PV systems with the response to grid disturbances (e.g. voltage sag) is the ability

to provide dynamic grid support in the form of Low-Voltage Ride-Through (LVRT) and Reactive Power Injection (RPI). Such grid requirements are already effective in some countries in order to: a) stabilize the grid in case of failures and b) to avoid loss of massive PV generation systems due to transients in the grid voltage. For instance, in Italy, any generation system with the total power exceeding 6 kW should have LVRT capability [21]. Other countries also keep the pace with grid code revision in order to accept more PV systems in the grid [10], [22]–[24]. Obviously, the implementation of LVRT function violates the anti-islanding requirement. Hence, as it is shown in Fig. 1, compatibility of those two functions should be taken into account when upgrading grid requirements.

Nonetheless, as the penetration level is continuously growing, the grid requirements for single-phase PV systems are going to be further enhanced, being more stringent and more specific in order to ensure a reliable and efficient power generation with reduced cost of energy. It is better for the next generation PV systems to have reactive power control function to support the grid voltage statically and also ride-through faults dynamically, which is associated with RPI control during the transients.

In the light of the above issues, RPI strategies for single-phase PV systems, specially in LVRT operation mode, are explored in this paper. Those proposed RPI strategies are: a) constant average active power control, b) constant active current control, c) constant peak current control and d) thermal optimized reactive power control strategy. To implement the discussed control strategies, a brief introduction of the power control for single-phase PV systems is given in § II. Verifications are first done for the thermal optimized control strategy on a 3 kW single-phase PV system by simulations, while the others are tested on a 1 kW singe-phase system in the LVRT operation mode. The results, which demonstrate the effectiveness of the proposed RPI strategies, are presented in § IV before the conclusions.

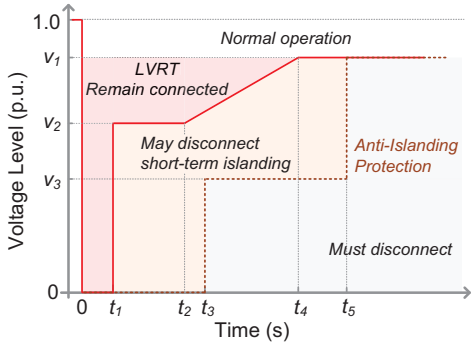

Fig. 1. Suggestion on a compatible implementation of low-voltage (and zero-voltage) ride-through and anti-islanding requirements for single-phase PV systems connected to low-voltage networks.

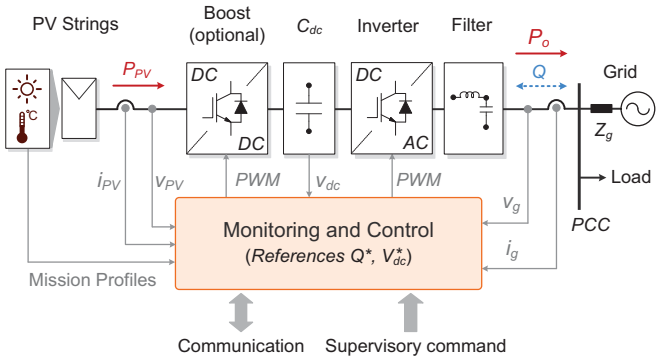

Fig. 2. Typical power and control configuration of a single-phase grid-connected PV system.

II. Power Control of Single-Phase Systems

Since the PV systems are still dominantly for residential applications at present, single-phase topologies are more widely-used solutions for PV systems. Fig. 2 represents a typical single-phase PV system connected to the grid through a string inverter. As it is shown in Fig. 2, in some cases, a DC-DC converter is adopted to boost up the PV panel voltage within an acceptable range of the PV inverter [6], [9], [25]. It also offers the flexibility of MPPT control, which is a basic requirement for such systems operating at unity power factor. Meanwhile, the injected current should be synchronized with the grid voltage. Besides, as mentioned previously, the system should disconnect from the grid when it presents disturbances (e.g. frequency or voltage variation) at the Point of Common Coupling (PCC) as shown in Fig. 2.

As for the control of single-phase systems with the RPI function, one possibility is based on the droop concept [8], [26], [27], which also requires that the line is mainly inductive (i.e. $X \gg R$). However, the single-phase distributed line has a lower X/R ratio, being mainly resistive. Hence, the droop control method for single-phase PV system to realize the RPI function is not suitable, while the utilization of adaptive filtering technique leads to an instantaneous power control solution [28]. This power control method is a good candidate for single-phase systems when a satisfactory synthesis of the power references is achieved. Besides the above control possibilities to achieve the RPI objective, the control system can also be developed in the $dq-$ or $\alpha\beta-$frame, based on the single-phase PQ theory [25], [28]–[31]. The implementation of this control solution is intuitive with less complexity, but it requires an Orthogonal Signal Generation (OSG) system to create quadrature components corresponding to the real grid voltage v_g and current i_g, as shown in Fig. 3. Moreover, a power calculation method in terms of fast computation and high accuracy can contribute to the control performance.

Thus, the RPI control can be implemented in this control solution by setting the reference active power P^* and reactive power Q^*, and then the grid current reference i_g^* is generated. In normal operation mode, the active power reference P^* is the tracked maximum power, P_{MPP}, of the PV panels ($P^* = P_{MPP}$) and $Q^* = 0$ Var. When the RPI control is enabled by a detected grid condition (voltage and frequency range), the reactive power is injected according to the grid requirements, e.g. E.ON. grid code shown in Fig. 4(a) [32].

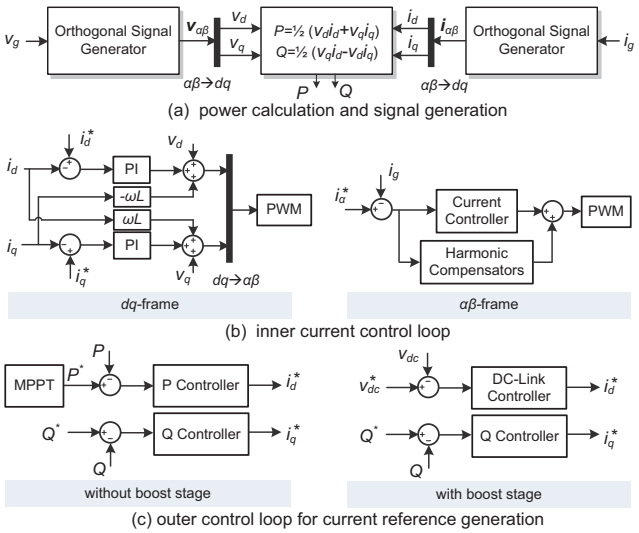

Fig. 3. Control structure for single-phase systems w/o boost converter based on single-phase PQ theory.

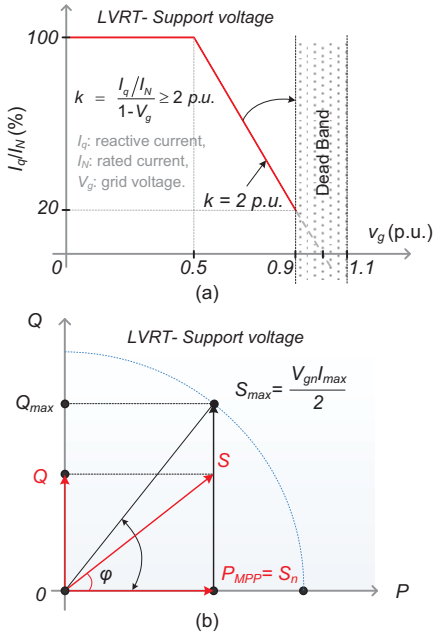

Fig. 4. Reactive power profiles for single-phase systems: (a) during LVRT required by E.ON. [32] and (b) reactive power capability of a PV inverter.

However, the amount of reactive power is limited by the inverter apparent power, S_{max}, as it is illustrated in Fig. 4(b). This constraint should be taken into account when designing the RPI strategies, i.e. the avoidance of inverter trip-off due to over-current protection.

III. Reactive Power Injection Strategies

Grid codes related to low-voltage applications are being under major revision [4], [10], [22], [23]. Some specifications have been imposed on the next-generation PV systems. In the future, PV systems, covering a wide range of applications, have to provide reactive power both in normal operation mode and under grid faults. Those features call for an emerging development of advanced PV inverters with reactive power control capabilities, including LVRT function with RPI control. Thus, in this section, considering the dynamic grid support requirement and the inverter maximum current limitation shown in Fig. 4, the following four strategies are explored in this paper:

A. Constant Average Active Power Control

The objective of this RPI control strategy is to maximize the output energy during LVRT operation. Therefore, the average active power is maintained constant. Based on the single-phase PQ theory, the average active power can be given as,

$$P = \frac{1}{2} v_g I_d \tag{1}$$

where v_g is the amplitude of the grid voltage and I_d is d-axis (active) current of the injected grid current. In the normal operation mode, $I_d = I_N$, and hence, under LVRT situation with constant average active power control, the average active power $P = P_N = \frac{1}{2} v_{gn} I_N$, with v_{gn} and I_N being the nominal values of the grid voltage and current, respectively.

According to the reactive power current requirements in Fig. 4(a) and (1), the current in the dq-rotating reference frame can be expressed as,

$$\begin{cases} I_d = & \dfrac{1}{v_g} I_N \\ I_q = & k(1 - v_g) I_N \end{cases} \tag{2}$$

in which $\left(1 - \frac{1}{k}\right)$ p.u $\leq v_g < 0.9$ p.u. is the instantaneous grid voltage level in p.u., and k is defined in Fig. 4(a). When the residual grid voltage is lower than $\left(1 - \frac{1}{k}\right)$ p.u., the system is required to fully inject reactive power while the active power output is disabled (i.e., $I_d = 0$ and $I_q = I_N$).

However, when the required injection of reactive power is fulfilled, it might pose the inverter at a risk of over-current and over-heating with this control strategy to maintain a constant output power. Thus, the following constraint should be satisfied in order to avoid inverter shutdown during LVRT:

$$\frac{1}{v_g} \sqrt{1 + k^2 (v_g - v_g^2)^2} \leq \frac{I_{max}}{I_N}, \tag{3}$$

where I_{max} is the inverter maximum allowable current. This could be the design criterion for component selection, and it can be further illustrated in Fig. 5.

It is observed in Fig. 5 that the minimum value of the inverter current limitation (I_{max}) should be $2.25 I_N$ so that the RPI strategy can be adopted in case of a wide range of voltage drop. As for a predesigned PV inverter with a robustness margin, the system has to derate the output power in order to inject enough reactive power. For example, the allowable maximum current of a PV inverter, $I_{max} = 1.5 I_N$ and k=2, the PV systems should reduce active power output, when the voltage drops below 0.72 p.u., as it is shown in Fig. 5. In that case, the system is not operating at this RPI control.

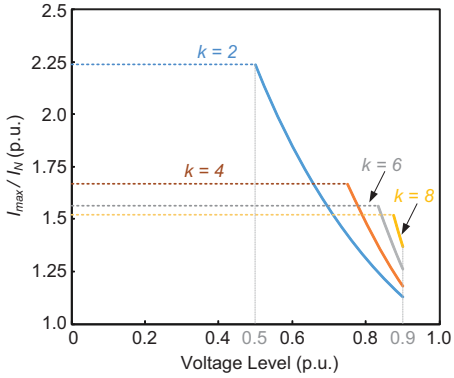

Fig. 5. Design constraint of the constant average active power control strategy considering the inverter over-current protection, where k is defined in Fig. 4(a).

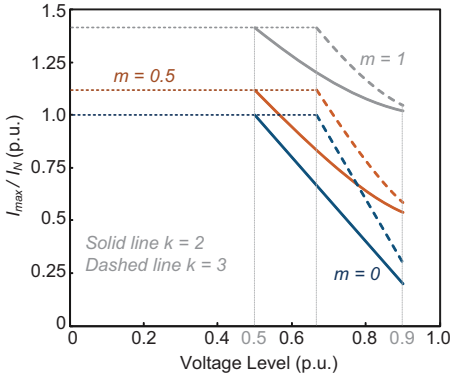

Fig. 6. Design constraint of the constant active current control strategy considering the inverter over-current protection, where $m = I_d/I_N$ and k is defined previously in Fig. 4(a).

B. Constant Active Current Control

Another RPI control possibility under LVRT operation is to keep the active current constant (i.e. $I_d = const.$). According to (1), the active current I_d can be obtained as,

$$I_d = \frac{2P}{v_g} = const. \tag{4}$$

Hence, the active power will automatically be reduced when this RPI control strategy is adopted in response to voltage sags, i.e. $P \propto v_g$. Meanwhile, the reactive current I_q can be calculated on the basis of the requirement shown in Fig. 4(a). Subsequently, the current in the dq-frame can be given as,

$$\begin{cases} I_d = & mI_N \\ I_q = & k(1-v_g)I_N \end{cases} \tag{5}$$

where v_g and k are defined previously, and $0 \leq m \leq 1$ is the active current level index corresponding to the nominal current I_N. Notably, when a severe voltage fault happens (very low voltage), the PV system should inject full reactive power without delivering active power to the grid. For simplicity, the level of active current can be controlled to be that of the rated current (i.e. $m = 1$, $I_d = I_N$).

With this RPI control strategy, the amplitude of the injected current, $I_{gmax} = \sqrt{I_d^2 + I_q^2}$, may also exceed the inverter limitation ($I_{gmax} > I_{max}$) and trip the inverter protection. In order to avoid this, the following condition should be fulfilled,

$$\sqrt{m^2 + k^2(1-v_g)^2} \leq \frac{I_{max}}{I_N}. \tag{6}$$

Similarly, a design guide for this RPI control strategy can be given in Fig. 6. It is seen from Figs. 5 and 6 that the PV inverter with constant active current control can be designed with a lower I_{max}/I_N when it is compared to the one with constant average active power control strategy. Therefore, it offers the possibilities to select power devices with lower current ratings and thus lower cost. It is also worth to point out that derating operation of a PV system can be achieved by changing m because of the proportional relationship between active power and voltage, $P \propto v_g$.

C. Constant Peak Current Control

A PV inverter with the previous discussed RPI strategies has a risk of over-current loading when it is operating in LVRT operation mode. Thus, the constant peak current control method is proposed. With this control strategy, there is no unintentional inverter shutdown due to over-current protection, since the peak of the injected grid current is kept constant and lower than the inverter current limitation during LVRT, i.e. $I_{gmax} = const. < I_{max}$. The injected reactive current (I_q) is calculated according to Fig. 4(a), and therefore the current under grid faults can be expressed as,

$$\begin{cases} I_d = & \sqrt{n^2 - k^2(1-v_g)^2}I_N \\ I_q = & k(1-v_g)I_N \end{cases} \tag{7}$$

where $1 \leq n \leq \frac{I_{max}}{I_N}$ is introduced as the peak current index corresponding to the nominal current I_N, and thus $I_{gmax} = nI_N$. Here, v_g and k are the same as previous definitions, and when $v_g < \left(1 - \frac{1}{k}\right)$ p.u., the full reactive power injection operation mode must be enabled.

The grid peak current I_{gmax} can be set as the rated current level I_N of the PV system, i.e. $n = 1$, $I_{gmax} = I_N$. By doing so, riding-through operation of the PV inverter will not give an amplitude rise to the injected grid current. Meanwhile, according to (1) and (7), the active power will be reduced in order to inject sufficient reactive power during LVRT.

D. Thermal Optimized Reactive Power Control Strategy

High efficiency and high reliability have become of intense importance for next-generation PV inverters in order to reduce the cost of energy [10], [33], [34]. Improvement of efficiency can be achieved by developing advanced power devices, and adopting transformerless inverters as proved by the European market [6], [30], [35]. Optimization of transformerless PV systems is another way to increase the efficiency [36]. In respect to reliability, possibilities to improve it can be achieved by considering rated power, packaging technologies, severe users, and harsh operation conditions, e.g. under grid faults [33], [34], [37], [38]. However, as shown in (8), the junction temperatures, including mean junction temperature, T_{j_m}, and

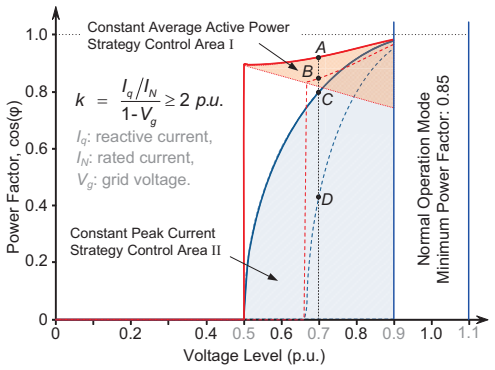

Fig. 7. Power factor curves vs. voltage levels for different control strategies: solid lines: k = 2 and dashed lines: k = 3.

temperature swings, ΔT_j, have a significant impact on the lifetime of a power device [39], and the entire system reliability.

$$N_f = \alpha \left(\Delta T_j\right)^{\beta_1} e^{\frac{\beta_2}{T_{j\text{-}m}}} t_{ON}^{\beta_3} i^{\beta_4} \tag{8}$$

with N_f being the the cycle-to-failure number, k, $\beta_{1,2,3,4}$ being the coefficients related to the device material, t_{ON} is the switching pulse width, and i being the wire current.

In LVRT operation, the injected reactive power is dependent on the voltage sag level, and also as shown in Fig. 4(a), k is variable. Both will lead to a redistribution of power losses, and thus thermal distribution, on the power devices. Therefore, a constant junction temperature (or at least cooled-down junction temperature) of the power devices, and thus improved overall reliability can be achieved by changing the RPI strategies and/or the slope k shown in Fig. 4(a). For example, as it is shown in Fig. 7, a voltage sag (0.3 p.u.) occurs and the constant peak current control strategy is firstly activated. By adjusting the value k to 3 p.u., the operation points will change from ***C*** to ***D***; while by changing the RPI strategy to constant average active power control, the operation point will correspondingly move from ***C*** to ***A***.

This is the basic operation principle of the thermal optimized reactive power control strategy. A detailed implementation of this control strategy is shown in Fig. 8, which shows that the thermal optimized reactive power control strategy complies with both RPI requirement in LVRT ("*Grid Requirements*" unit) and improved reliability demand ("*Thermal Optimization*" unit). In normal operation mode, since a minimum power factor is required, the system only sets the references (P_L^* and Q_L^*) for the central control unit; while in the case of a voltage sag both control units will send out the power references (P_L^* and Q_L^*, P_j^* and Q_j^*), and then central control unit will optimize the power to achieve both goals. Thus, the optimization function can simply be expressed as,

$$\{P^*, Q^*\} = f_{opti}\left(P_L^*, Q_L^*, P_j^*, Q_j^*\right). \tag{9}$$

Fig. 9 presents an example of a PV inverter to keep the maximum junction temperature constant with the proposed strategy. Together with the active and reactive power references in the other three RPI strategies, the thermal optimized

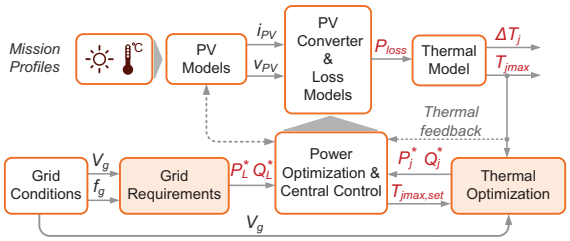

Fig. 8. Control structure of thermal optimized reactive power control strategy for single-phase PV systems.

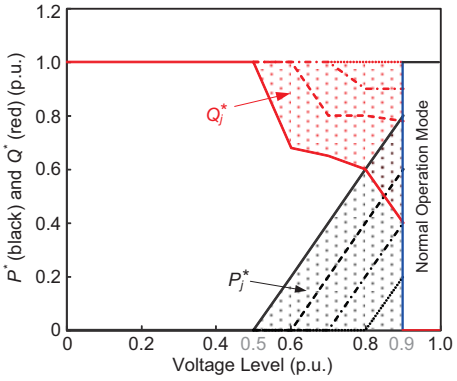

Fig. 9. Active power and reactive power references for a 3 kW single-phase PV system with thermal optimized control to achieve a constant junction temperature on the IGBTs.

reactive power control strategy can be implemented in Fig. 8 and optimized based on (9). However, it should be pointed out that a voltage fault normally is a very short term event, and thus the thermal optimized control strategy may not take a fast and effective response to the voltage sag during this time interval. Yet, the idea of thermal optimization by reallocating the active power and reactive power can be adopted in the power electronics based systems in order to achieve improved reliability, and thus a reduced cost of energy.

Nevertheless, during the design and the operation of the PV inverters, those above constraints should be considered. Especially, for the next generation PV systems, the provision of reactive power as an advanced feature both in normal operation and under grid faults, and the requirements of LVRT will come into force in the near future. The corresponding active and reactive power references under different voltage sag levels for the proposed RPI control strategies can be obtained based on the above discussions. Thus, the required reactive power complying with grid codes can be injected.

IV. Simulation and Experimental Results

Referring to Fig. 2, simulation and experimental tests were carried out to demonstrate the effectiveness of the proposed RPI control strategies. Fig. 10 shows the hardware configuration of a single-phase system used for the verifications, and it also shows that the RPI control strategies triggered by voltage variations will set the power references for the power controller. System parameters are listed in Table I.

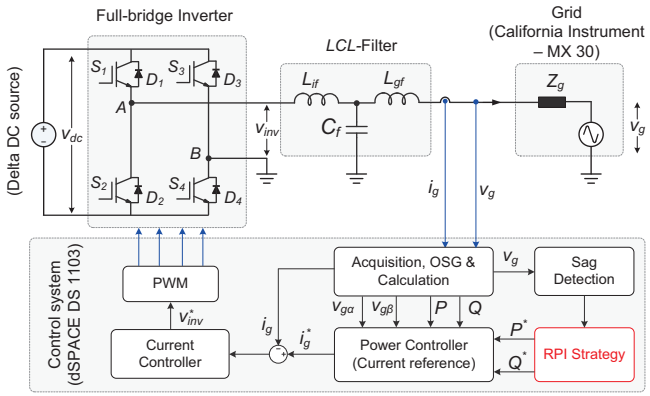

Fig. 10. Hardware schematic and overall control structure of a single-phase system with RPI control strategies based on the single-phase PQ theory.

TABLE I

SIMULATION AND EXPERIMENTAL PARAMETERS.

Nominal Grid Amplitude	$v_{gn} = 230\sqrt{2}$ V
Nominal Grid Frequency	$\omega_0 = 2\pi \times 50$ rad/s
Grid Impedance	L_g= 50 μH, R_g= 0.2 Ω
LCL-Filter	L_{if}= 3.6 mH, C_f =2.35 μF, L_{gf}= 708 μH
Sampling and Switching Frequency	$f_s = f_{sw}$= 10 kHz
DC Voltage	V_{dc}=400 V

In both simulations and experiments, a proportional resonant current controller with harmonic compensations is adopted to maintain a satisfactory power quality. The power controller is implemented in the $\alpha\beta$-frame according to Fig. 3.

Simulations are firstly carried out. Fig. 11 shows the performance of a 1 kW single-phase system with constant peak current, constant active current, and constant average power RPI strategies in LVRT. Based on the thermal models in [38], [40] and thermal parameters of the IGBT module (Table II), a 3 kW single-phase system with the thermal optimized RPI control strategy is simulated and the results are given in Fig. 12. During LVRT operation, the system injects the required reactive power to support the voltage, and at the same time, the active power is also controlled in order to achieve different objectives, e.g. maintain the peak current and stabilize the junction temperature of the power devices as demonstrated in Figs. 11 and 12. Notably, with the thermal optimized control strategy, the junction temperature of IGBT power devices is maintained constant while sufficient reactive power is also injected to the grid. Hence, both required reactive power support and improved reliability are achieved.

In the experimental verifications, a voltage sag of 120 ms is programmed in the California Instruments AC power source. The constant average active power control strategy has been tested firstly on a 1 kW system. Since a three-phase commercial inverter has been used as the conversion stage,

TABLE II

THERMAL PARAMETERS OF THE IGBT MODULE FROM A LEADING MANUFACTURER FOR THE SIMULATIONS.

Impedance		$Z_{th(j-c)}$, Junction-to-case temp.			
i		1	2	3	4
IGBT	R_{thi} (K/W)	0.074	0.173	0.526	0.527
	τ_i (s)	0.0005	0.005	0.05	0.2
Diode	R_{thi} (K/W)	0.123	0.264	0.594	0.468
	τ_i (s)	0.0005	0.005	0.05	0.2

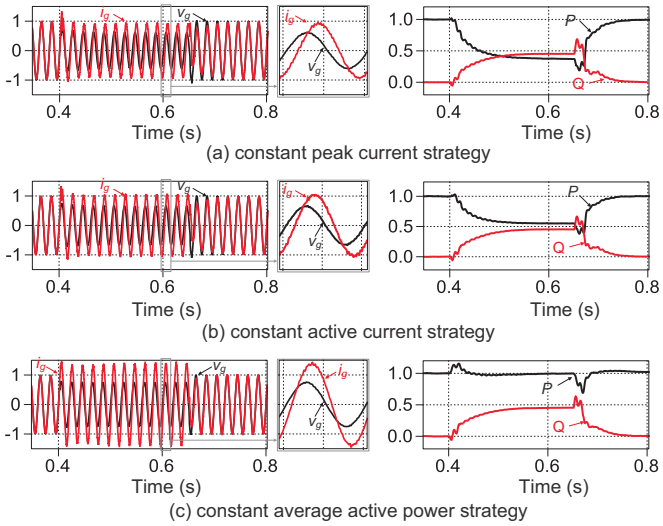

Fig. 11. Performance of a single-phase 1 kW PV system in LVRT operation mode with three different RPI control strategies: i_g, v_g- grid current and voltage [p.u.]; P, Q- average active power reactive power [p.u.]; voltage sag level: 0.45 p.u..

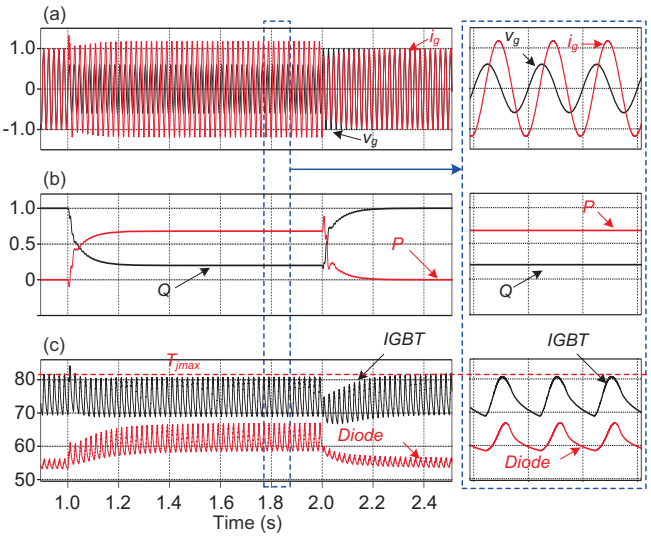

Fig. 12. Simulation results of a 3 kW single-phase PV system with thermal optimized reactive power control strategy: (a) grid current and voltage i_g, v_g [p.u.], (b) active and reactive power P, Q [p.u.] and (c) junction temperature T_j [°C]; voltage sag level: 0.45 p.u..

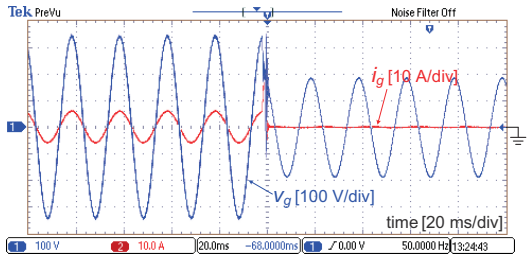

Fig. 13. Over-current protection of a single-phase system with constant average active power control (0.45 p.u. voltage sag).

the rated current is 5 A in RMS per phase. If a severe voltage fault (e.g. 0.45 p.u.) happens, the amplitude of the injected grid current may exceed the current limitation, and consequently, the inverter will be tripped off, as it is shown in Fig. 13. One possibility is to reduce the output power (change m) as discussed previously. Here, in the experimental results shown in Fig. 14, the voltage presents a 0.22 p.u. voltage sag, and thus the system can inject sufficient reactive power injection without derating active power.

By contrast, the constant peak current and constant active current control strategies are tested under a severe voltage sag (0.45 p.u.) on the same system. The performance of the single-phase system under such a voltage fault is shown in Fig. 15. The results demonstrate that the constant peak current control strategy can contribute to a constant amplitude of the injected current and at the same time an injection of appropriate reactive power. Similarly, the constant active current RPI strategy can inject sufficient reactive power, which is dependent on the voltage sag level, and the active current is maintained constant during LVRT operation.

V. Conclusion

In this paper, reactive power injection strategies for single-phase PV systems considering grid requirements have been explored. The proposed reactive power injection strategies include constant average active power control, constant active current control, constant peak current control, and thermal optimized reactive power control strategy, which is dedicated to improve the reliability during LVRT operation. All the discussed control strategies are in compliance with the grid codes. The proposed reactive power control strategies have also been tested either by simulations or by experiments. The results show the effectiveness of the reactive power injection strategies to support the grid voltage during LVRT operation with different objectives, e.g. maximum output power (constant average active power control). Design constraints for those strategies have also been studied in this paper. As the future grid demands will be more stringent, and the reactive power injection function is one of them, the PV systems serving even low-voltage grids have to comply with those requirements. The proposed control strategies can be implemented in those PV systems with the provided design guidelines. Hence, the control strategies can further accelerate the pace of advanced PV inverter development.

References

[1] C. Winneker, "Worlds solar photovoltaic capacity passes 100-gigawatt landmark after strong year," [Online]. Available: http://www.epia.org/news/, Feb. 2013.

[2] D. Rosenwirth and K. Strubbe, "Integrating variable renewables as Germany expands its grid," [Online]. Available: http://www.renwableenergyworld.com/, Mar. 2013.

[3] European Photovoltaic Industrial Association, "Global market outlook for photovoltaics until 2016," [Online]. Available: http://www.epia.org/, 2012.

[4] Y. Bae, T.-K. Vu, and R.-Y. Kim, "Implemental control strategy for grid stabilization of grid-connected PV system based on German grid code in symmetrical low-to-medium voltage network," *IEEE Trans. Energy Conversion*, vol. 28, no. 3, pp. 619–631, Sept. 2013.

[5] REN 21, "Renewables 2013: Global Status Report (GSR)," [Online]. Available: http://www.ren21.net/, Jun. 2013.

[6] S.B. Kjaer, J.K. Pedersen, and F. Blaabjerg, "A review of single-phase grid-connected inverters for photovoltaic modules," *IEEE Trans. Ind. Appl.*, vol. 41, no. 5, pp. 1292–1306, Sept./Oct. 2005.

[7] F. Blaabjerg, R. Teodorescu, M. Liserre, and A.V. Timbus, "Overview of control and grid synchronization for distributed power generation systems," *IEEE Trans. Ind. Electron.*, vol. 53, no. 5, pp. 1398–1409, Oct. 2006.

[8] Y. Yang, F. Blaabjerg, and Z. Zou, "Benchmarking of grid fault modes in single-phase grid-connected photovoltaic systems," *IEEE Trans. Ind. Appl.*, vol. 49, no. 5, pp. 2167–2176, Sept./Oct. 2013.

[9] E. Romero-Cadaval, G. Spagnuolo, L. Garcia Franquelo, C.A. Ramos-Paja, T. Suntio, and W.M. Xiao, "Grid-connected photovoltaic generation plants: Components and operation," *IEEE Ind. Electron. Mag.*, vol. 7, no. 3, pp. 6–20, 2013.

[10] Y. Yang, P. Enjeti, F. Blaabjerg, and H. Wang, "Suggested grid code modifications to ensure wide-scale adoption of photovoltaic energy in distributed power generation systems," in *Proc. of IEEE-IAS Annual Meeting*, pp. 1-8, 6-11 Oct. 2013.

[11] R. Teodorescu, M. Liserre, and P. Rodriguez, *Grid converters for photovoltaic and wind power systems*. Hoboken, NJ, USA: Wiley, 2011.

[12] M. Ciobotaru, R. Teodorescu, and F. Blaabjerg, "Control of single-stage single-phase PV inverter," in *Proc. of EPE'05*, pp. P.1-P.10, 2005.

[13] S. Jain and V. Agarwal, "A single-stage grid connected inverter topology for solar PV systems with maximum power point tracking," *IEEE Trans. Power Electron.*, vol. 22, no. 5, pp. 1928–1940, Sept. 2007.

[14] E.J. Coster, J.M.A. Myrzik, B. Kruimer, and W.L. Kling, "Integration issues of distributed generation in distribution grids," *Proceedings of the IEEE*, vol. 99, no. 1, pp. 28–39, 2011.

[15] H. Gaztanaga, J. Landaluze, I. Etxeberria-Otadui, A. Padros, I. Berazaluce, and D. Cuesta, "Enhanced experimental PV plant grid-integration with a MW Lithium-Ion energy storage system," in *Proc. of ECCE*, pp. 1324-1329, 15-19 Sept. 2013.

[16] G. Mokhtari, A. Ghosh, G. Nourbakhsh, and G. Ledwich, "Smart robust resources control in LV network to deal with voltage rise issue," *IEEE Trans. Sustain. Energy*, vol. 4, no. 4, pp. 1043–1050, 2013.

[17] T. Stetz, F. Marten, and M. Braun, "Improved low voltage grid-integration of photovoltaic systems in Germany," *IEEE Trans. Sustain. Energy*, vol. 4, no. 2, pp. 534–542, 2013.

[18] R. Caldon, M. Coppo, and R. Turri, "Distributed voltage control strategy for LV networks with inverter-interfaced generators," *Electric Power Systems Research*, vol. 107, pp. 85–92, 2014.

[19] M. Arnold, W. Friede, and J. Myrzik, "Challenges in future distribution grids - A review," in *Proc. of ICREPQ'13*, pp. 1-6, 20-22 Mar. 2013.

[20] VDE Verband der Elektrotechnik Elektronik Informationstechnik e.V., "Power generation systems connected to the low-voltage distribution network - Technical minimum requirements for the connection to and parallel operation with low-voltage distribution networks," *VDE-AR-N 4105:2011-08*, Aug. 2011.

[21] Comitato Elettrotecnico Italiano, "Reference technical rules for connecting users to the active and passive LV distribution companies of electricity," *CEI 0-21*, Dec. 2011.

[22] H. Kobayashi, "Fault ride through requirements and measures of distributed PV systems in Japan," in *Proc. of IEEE-PES General Meeting*, pp. 1-6, 22-26 Jul. 2012.

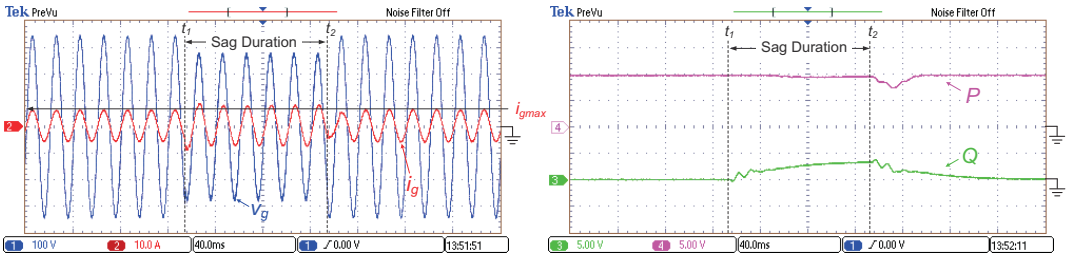

Fig. 14. Experimental results of a single-phase system with constant average active power RPI control strategy (0.22 p.u. voltage sag): grid voltage v_g [100 V/div], grid current i_g [10 A/div], active power P [500 W/div], reactive power Q [500 Var/div], and time [40 ms/div].

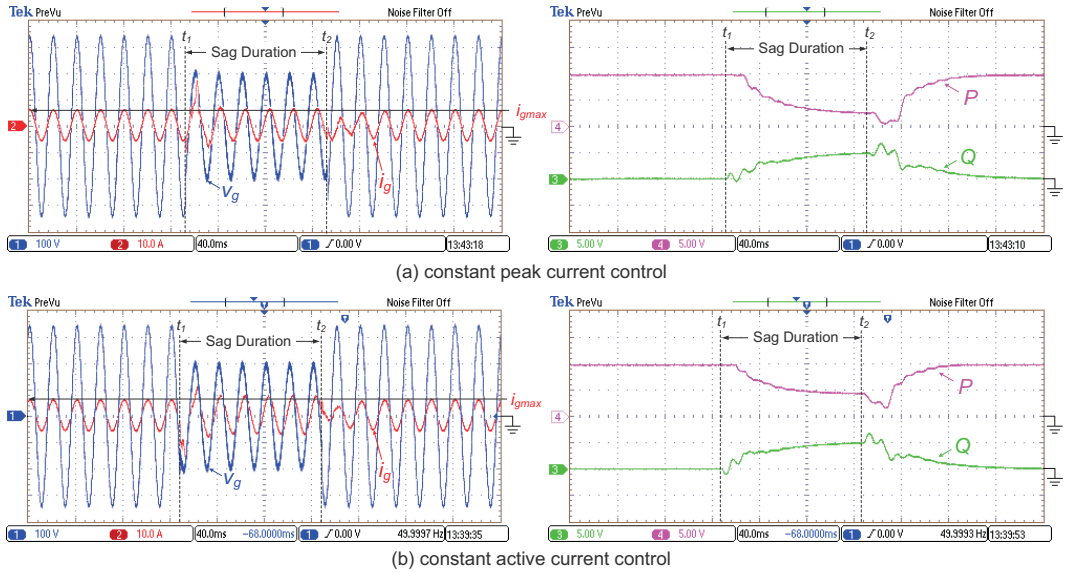

Fig. 15. Experimental results of a single-phase system with constant peak current and constant active current RPI control strategies (0.45 p.u. voltage sag): grid voltage v_g [100 V/div], grid current i_g [10 A/div], active power P [500 W/div], reactive power Q [500 Var/div], and time [40 ms/div].

[23] N. Papanikolaou, "Low-voltage ride-through concept in flyback inverter-based alternating current- photovoltaic modules," *IET Power Electron.*, vol. 6, no. 7, pp. 1436–1448, Aug. 2013.

[24] Y. Miyamoto, "Technology for high penetration residential PV systems on a distribution line in Japan," in *Proc. of the fifth Int'l Conf. on Integration of Renewable and Distibuted Energy Resources*, 4-6 Dec. 2012.

[25] R. Carnieletto, D.I. Brandao, F.A. Farret, M.G. Simoes, and S. Suryanarayanan, "Smart grid initiative: A multifunctional single-phase voltage source inverter," *IEEE Ind. Appl. Mag.*, vol. 17, no. 5, pp. 27–35, 2011.

[26] L.P. Sampaio, M.A.G. de Brito, G. de Azevedo e Melo, and C.A. Canesin, "Power flow control in single-phase and three-phase grid-connected inverters using LMI, state-feedback linearization and D-stability," in *Proc. of EPE'13*, pp. 1-10, 2013.

[27] H.J. Avelar, W.A. Parreira, J.B. Vieira, L.C.G. de Freitas, and E.A. Alves Coelho, "A state equation model of a single-phase grid-connected inverter using a droop control scheme with extra phase shift control action," *IEEE Trans. Ind. Electron.*, vol. 59, no. 3, pp. 1527–1537, 2012.

[28] S.A. Khajehoddin, M. Karimi-Ghartemani, A. Bakhshai, and P. Jain, "A power control method with simple structure and fast dynamic response for single-phase grid-connected DG systems," *IEEE Trans. Power Electron.*, vol. 28, no. 1, pp. 221–233, 2013.

[29] C.-H. Chang, Y.-H. Lin, Y.-M. Chen, and Y.-R. Chang, "Simplified reactive power control for single-phase grid-connected photovoltaic inverters," *IEEE Trans. Ind. Electron.*, vol. 61, no. 5, pp. 2286–2296, 2014.

[30] Y. Yang, F. Blaabjerg, and H. Wang, "Low voltage ride-through of single-phase transformerless photovoltaic inverters," *IEEE Trans. Ind. Appl.*, vol. 0, no. 99, pp. 1–8, May/Jun. in press, 2014.

[31] M. Jang, M. Ciobotaru, and V.G. Agelidis, "A single-phase grid-connected fuel cell system based on a boost-inverter," *IEEE Trans. Power Electron.*, vol. 28, no. 1, pp. 279–288, 2013.

[32] E.ON GmbH, "Grid Code-high and extra high voltage," 2006.

[33] H. Wang, M. Liserre, and F. Blaabjerg, "Toward reliable power electronics: Challenges, design tools, and opportunities," *IEEE Ind. Electron. Mag.*, vol. 7, no. 2, pp. 17–26, 2013.

[34] H. Huang and P. Mawby, "A lifetime estimation technique for voltage source inverters," *IEEE Trans. Power Electron.*, vol. 28, no. 8, pp. 4113–4119, 2013.

[35] I. Patrao, E. Figueres, F. Gonzlez-Espn, and G. Garcer, "Transformerless topologies for grid-connected single-phase photovoltaic inverters," *Renewable and Sustainable Energy Reviews*, vol. 15, no. 7, pp. 3423 – 3431, 2011.

[36] E. Koutroulis and F. Blaabjerg, "Design optimization of transformerless grid-connected PV inverters including reliability," *IEEE Trans. Power Electron.*, vol. 28, no. 1, pp. 325–335, 2013.

[37] Y. Xue, K.C. Divya, G. Griepentrog, M. Liviu, S. Suresh, and M. Manjrekar, "Towards next generation photovoltaic inverters," in *Proc. of ECCE*, pp. 2467-2474, 17-22 Sept. 2011.

[38] Y. Yang, H. Wang, F. Blaabjerg, and K. Ma, "Mission profile based multi-disciplinary analysis of power modules in single-phase transformerless photovoltaic inverters," in *Proc. of EPE'13 ECCE Europe*, pp. 1-10, 2-6 Sept. 2013.

[39] D. Wagenitz, A. Hambrecht, and S. Dieckerhoff, "Lifetime evaluation of IGBT power modules applying a nonlinear saturation voltage observer," in *Proc. CIPS 2012*, pp. 1-5, Mar. 2012.

[40] Plexim GmbH, "PLECS User Manual Version 3.4," [Online]. Available: http://www.plexim.com/, 14 Jun. 2013.